Published in final edited form as:
J Comp Neurol. 2009 October 20; 516(6): 569–579. doi:10.1002/cne.22117.

Connexin30 null and conditional connexin26 null mice display distinct pattern and time course of cellular degeneration in the cochlea

Yu Sun[1,3], **Wenxue Tang**[1], **Qing Chang**[1], **Yunfeng Wang**[1], **Weijia Kong**[3,*], and **Xi Lin**[1,2,*]

[1]Department of Otolaryngology, Emory University School of Medicine, 615 Michael Street, Atlanta, GA 30322-3030, USA.

[2]Department of Cell Biology, Emory University School of Medicine, 615 Michael Street, Atlanta, GA 30322-3030, USA.

[3]Department of Otolaryngology, Union Hospital, Tongji Medical College, Huazhong University of Science and Technology, Wuhan 430022, PR China.

Abstract

Mutations in connexin26 (Cx26) and Cx30 are the most common cause of non-syndromic inherited deafness in humans. To understand underlying molecular mechanisms, we investigated the pattern and time course of cellular degeneration in the cochlea of conditional Cx26 (cCx26) null and Cx30 null mice. In cCx26 null mice, initial degeneration was observed around postnatal day 14 in outer hair cells (OHCs) and supporting cells surrounding the OHCs. All cells in the middle turn organ of Corti were lost one month after birth and degeneration gradually spread to the basal and apical turns. Most spiral ganglion (SG) neurons in the middle and basal turns disappeared in the first three months, while significant amounts of apical SG neurons survived. In the cochlea of Cx30 null mice, survival of most inner HCs, supporting cells and SG neurons was observed for up to eighteen months. The most severe degeneration was found in apical SG neurons and OHCs. OHC loss followed a slow time course and a base to apex gradient. Gross structures of the endolymphatic space and stria vascularis observed at the light microscope level were unchanged in either Cx null mouse models.

This study revealed that cellular degeneration in the cochlea of cCx26 null mice was dramatically more rapid and widespread than that observed in Cx30 null mice. The radically different pathogenesis processes displayed by cCx26 and Cx30 null mice suggest heterogeneous underlying deafness mechanisms, despite of the coassembly of Cx26 and Cx30 in forming gap junctions in the cochlea.

Keywords

neuronal degeneration; connexin26 mutation; connexin30 mutation; spiral ganglion neuron; hair cells; mouse model; genetic deafness

[*]**Co-correspondence authors:** (1) Xi Lin, PhD, Departments of Otolaryngology and Cell Biology, Emory University School of Medicine, Atlanta, GA 30322. Telephone: 404-727-3723, Fax: 404-727-6256, xlin2@emory.edu, and (2) Weijia Kong, Department of Otolaryngology, Union Hospital, Tongji Medical College, Huazhong University of Science and Technology, 430022 Wuhan, PR China. Telephone: 86-27-85726900, Fax: 86-27-85776343, wjkong@whuh.com.

Introduction

Connexins (Cxs) are building blocks of gap junctions (GJs), which are intercellular membrane channels facilitating exchanges of ions and small molecules (molecular weight <1k dalton) required for cellular signaling and homeostasis. The Cx gene family has twenty-one and twenty members in human and mouse genomes, respectively (Willecke et al., 2002). Different Cx protein subunits are conventionally named by adding a number that corresponds to their molecular weight (e.g., Cx26). Six compatible Cx subunits assemble into a hexmer in the cell membrane to form a GJ hemichannel. Two hemichannels in adjacent cells align to form a complete GJ channel that directly connects the cytoplasm of two cells when the GJ channel is open. Cx26 and Cx30 are the two predominant Cx subunits in the cochlea, and most cochlear GJs are formed by the coassembly of the two Cx subtypes (Ahmad et al., 2003; Forge et al., 2003). Genetic linkage studies have identified that mutations in genes coding for Cx26 (*GJB2*) (Kelsell et al., 1997) and Cx30 (*GJB6*) (Grifa et al., 1999) are responsible for deafness in a significant proportion of patients (30–50%) in most ethnic groups suffering from prelingual severe-to-profound nonsyndromic hearing loss (Chang et al., 2003; Denoyelle et al., 1997). cCx26 null (Cohen-Salmon et al., 2002) and Cx30 null mutant (Teubner et al., 2003) mice are profoundly deaf. It is well established that normal functions of Cx26 and Cx30 are essential for hearing, although mechanisms underlying the deafness caused by Cx mutations are not clear.

HCs in the cochlea degenerate in both Cx30 and cCx26 null mice (Cohen-Salmon et al., 2002; Teubner et al., 2003). Spiral ganglion (SG) neurons in the cochlea usually die after the loss of HCs. The cochlear implant is the most effective treatment for sensorineural deafness patients, including Cx mutation patients (Cullen et al., 2004). This prosthetic device provides auditory cues by directly stimulating SG neurons, thus bypassing the damaged or missing hair cells (HCs). Speech perception in many patients is restored without relying on lip reading (Skinner et al., 1997; Waltzman et al., 1997). However, outcomes of the performance among patients received cochlear implants have a wide spectrum. Since functionally-excitable SG neurons are required for the cochlear implant to work, a significant loss of SG neurons below a critical level may have a detrimental effect on the prognosis of the cochlear implant surgery (Clopton et al., 1980; Incesulu and Nadol, 1998). The HCs are the primary source of neurotrophic support for the SG neurons (Ernfors et al., 1995; Schecterson and Bothwell, 1994; Ylikoski et al., 1993). It is known that death of HCs caused by either noise damage or ototoxic drugs triggers degeneration of SG neurons (Leake and Hradek, 1988; Otte et al., 1978). However, how the time course and pattern of cellular degeneration differ in the cochlea of two Cx null mouse models is unclear. More importantly, whether genetic mutations in Cx26 and Cx30 genes affect the survival of SG neurons in the cochlea has not been examined yet. We therefore investigated the time course and pattern of cellular degeneration in the cochlea of cCx26 null and Cx30 null mice.

Materials and Methods

Mouse models

The animal use protocol in this study was approved by the Emory Institutional Animal Care and Use Committee. Cx30 null ($Gjb6^{-/-}$) and $Cx26^{loxP/loxP}$ mice were obtained from the European Mouse Mutant Archive (EMMA, http://www.emmanet.org/) with the written permission of Dr. Willecke. The Cx30 null mice were originally generated in a mixed 129P2/OlaHsd and C57BL/6NCrl genetic background (Teubner et al., 2003). It is known that wild type (WT) mice in C57BL genetic background display early-onset age-dependent hearing loss. In contrast, the CBA/CaJ mice show minimal age-dependent hearing loss (Zheng et al., 1999). To facilitate a long-term (>1 year) study of cochlear morphology, we transferred the $Gjb6^{-/-}$ genotype into a CBA/CaJ genetic background by backcrossing for

>8 generations. Genotype protocol used in this study for Cx30 null mice was the same as that described previously (Teubner et al., 2003).

Homozygous deletion of the gene for Cx26 in mice (*Gjb2*$^{-/-}$) is embryonically lethal due to the defect in glucose transportation across the placenta (Gabriel et al., 1998). To obtain a mouse model for human deafness caused by Cx26 null mutation, we didn't remove the *Gjb2* gene until after embryonic day 19 (E19) by a single injection of 4-hydroxytamoxifen (HTMX, Sigma, catalog# H7904, St. Louis, MO) to the dams (1 mg per 10g body weight, intraperitoneal (I.P.)). We found that injection of HTMX earlier than E19 was still lethal to the embryos. The cCx26 mutant mouse model was generated by cross breeding two kinds of genetically-modified mice: (1) Mice in which both copies of the *Gjb2* gene are flanked by the loxP sequence (Cx26$^{loxP/loxP}$ mice). The exon2 of the *Gjb2*, which is the entire coding region for Cx26, is flanked by the loxP sequences in the Cx26$^{loxP/loxP}$ mice. Therefore, activation of Cre recombinase is expected to remove the entire coding sequence of Cx26. Previous studies show that the hearing of Cx26$^{loxP/loxP}$ mice is normal (Cohen-Salmon et al., 2002); (2) R26cre-ER^{T} mice (Vooijs et al., 2001) that also carried the loxP sequence around the *Gjb2* (Cx26$^{loxP/loxP}$;Rosa26^{CreER} mice). The original R26cre-ER^{T} mice (Gt(ROSA)26Sor$^{(cre/Esr1)Nat}$, Stock number 004453) were purchased from the Jackson Laboratory (Bar Harbor, ME). In the R26cre-ER^{T} mice, a ligand-dependent Cre recombinase coded by a fusion gene encoding Cre and the mutated (G521R) ligand binding domain of the estrogen receptor was expressed ubiquitously from the Rosa26 locus. The Cre is activated in the presence of the synthetic estrogen antagonist HTMX (Vooijs et al., 2001). In our studies, all Cx26$^{loxP/loxP}$;Rosa26^{CreER} mice displayed nonsyndromic deafness and cellular degenerations after the HTMX injection. Mice that received HTMX injections but didn't carry the CreER (Cx26$^{loxP/loxP}$ without Rosa26^{CreER}) were used as littermate controls in functional and morphology studies.

Primer pairs used to detect the loxP sequences are: forward 5'-ACAGAAATGTGTTGGTGATGG-3'; reverse 5'-CTTTCCAATGCTGGTGGAGTG-3'. Cx26$^{loxP/loxP}$ and the wild type (WT) mice generated a band of 322 bps and 288 bps, respectively. The larger band was caused by the insertion of the 34 bp of the loxP sequence around the *Gjb2* gene. The presence of CreER was detected by using the primer pair: forward 5'-AGCTAAACATGCTTCATCGTCGGTC-3'; and reverse 5'-TATCCAGGTTACGGATATAGTTCATG-3', which gave rise to a PCR product of 700 bps. PCR protocol was: 95°C for 5 minutes, 35 cycles of 95°C for 1 minute, 55°C for 1 minute, 72°C for 1 minute.

Cre reporter mice (R26R mice) are widely used to monitor tissue specific Cre activation (Soriano, 1999). R26R mice express β-galactosidase after a Cre-mediated excision of a neo cassette. We crossed R26cre-ER^{T} mice with R26R mice (Jackson Laboratory, Bar Harbor, ME) to generate R26R;R26cre-ER^{T} mice. Because of the irreversible Cre-loxP excision, all cells in which the Cre recombinase is activated anytime during development express the reporter gene in all their lineages. Therefore, LacZ staining shows the cellular patterns of activation of Cre recombinase in the cochlea induced by HTMX injections. Primer pairs used for genotyping the R26R mice were: forward 5'-GATTGAAGCAGAAGCCTGCGATGTCGGTTT-3'; reverse 5-TGACGGAACAGGTATTCGCTGGTCACTTC-3'. The expected PCR product size is 972 bps. Same PCR thermocycle protocol as that used for detecting loxP and CreER was used. The standard protocol for LacZ staining was used (Soriano, 1999) on the cochlear samples. Cryosections with a thickness of 8 μm were cut (Leica CM1850, Germany) from these cochleae in order to better observe cellular patterns of LacZ staining.

Immunolabeling and resin cochlear section methods

Details of the immunolabeling protocol were given in our previously-published paper (Sun et al., 2005). Briefly, Cryo-cochlear sections cut at a thickness of 8 μm using a Cryostat (Leica CM1850, Germany) and whole-mount cochlear samples were permeablized with Triton (0.1% in PBS, pH 7.4) for 30 minutes. Nonspecific labeling was blocked with 10% goat serum in PBS at room temperature for 1 hr. Polycolonal antibodies against Cx26 and Cx30 were purchased from Invitrogen Corp (Carlsbad, CA), and catalog numbers are 13–8100 (lot#441118A) and 71–2200 (lot#354025A) respectively. These Cx antibodies were raised in either rabbit (71–2200) or mouse (13–8100) using synthetic peptides as antigens. Cx26 antigenic peptide sequence was selected from the unique sequence in the cytoplasmic loop of the protein, which was RRHEKKRKFMKGEIK. Cx30 antigenic peptide sequence was selected in the C-terminal unique to the Cx30, which was: SKRTQAQRNHPNHALKESKQNEMNELISDSGQNAITSFPS. Western blot characterization and controls for the two antibodies were published previously (Ahmad et al., 2003). Western blots in the current study again showed that both antibodies recognized a single band on Western blots at the expected molecular weights (Fig. 2A). The Cx30 and Cx26 immunoreactivities either disappeared in $Cx30^{-/-}$ mice (Ahmad et al., 2007) or greatly reduced in cCx26 null mice as expected (Fig. 2). These data supported that the binding of the two antibodies was specific to their intended target proteins.

The stock solution was diluted at 1:200 and samples were incubated at 4°C overnight. Cx26 labeling was visualized by using a donkey anti-mouse antibody conjugated to Rhodamine (1:200 dilution, Jackson ImunoResearch Lab Inc., catalog# 715-295-140, lot#68472). Alexa Fluor 488 secondary antibody (Invitrogen, Eugene, OR), which is a goat anti-rabbit IgG antibody, was used to visualize the Cx30 labeling (1:500 dilution. Labeling duration of both secondary antibodies was 1 hr at room temperature. Cochlear sections were also counterstained with 4',6-diamidino-2-phenylindole (DAPI, purchased from Molecular Probes, Eugene, OR, catalog#: D1306) to reveal the location of cell nuclei. Processed samples were mounted in antifade solution (Fluoromount-G, Electron Microscopy Sciences) and examined using a confocal microscope (Zesis LSM, Carl Zeiss USA). Narrow-band emission filter settings at 510–530nm and 560–580nm were used for the green and red channel, respectively.

For obtaining epoxy resin cochlear sections, we fixed cochleae first through cardioperfusion of 4% paraformaldehyde (in PBS). The cochlea was dissected out and postfixed in 1% osmium for 1 hr at room temperature. Samples were decalcified in 0.35 M EDTA (pH 7.5, in PBS) for 72 hrs at 4°C, followed by gradual dehydration in alcohol of increasing grades, infiltrated, and embedded in epoxy resin with the conventional protocols. Consecutive cochlear sections (5 μm in thickness) were stained with toluidine blue. For counting the SG neurons, two neighboring sections separated by 40 μm were used to eliminate the possibility of double counting because they should contain no SG neurons in common. No shrinkage of the soma of SG neurons was observed in the Cx mutant mice, therefore a straightforward point-counting method (Leake and Hradek, 1988) was used to estimate SG neuron density. The area of the Rosenthal's canal was measured with NIH ImageJ software from the cochlear sections. Final figures were compiled and edited with Photoshop (Adobe Systems Incorporated, San Jose, CA). The brightness and contrast of some of the image panels were adjusted for better clarity. No other photo manipulations were done to enhance the pictures. The number of SG neurons in the section was divided by the area of the Rosenthal's canal to obtain the density of SG neurons. Counting errors were corrected by using the Abercrombie's equation (Guillery, 2002): T/T+h, in which T is the section thickness and h is the mean diameter of the SG neurons. The student t-test was used to determine the significance of differences between various groups, and a p-value of <0.05 was used. Details

of the testing methods for auditory brainstem responses (ABRs) are given in our previously published papers (Ahmad et al., 2007).

To obtain cochleogram, whole-mount cochlea were dissected out and cut into apical, middle and basal turn pieces. The samples were stained with DAPI and non-confocal fluorescent images of each cochlear turns were taken with an inverted microscope (Zeiss Axiovert 135TV, Carl Zeiss, Germany). Nuclei of hair cells (examples are given by arrows in Fig. 7A&K) are counted. Loss of hair cells in specific location is expressed as percentage of time-matched WT controls at the same cochlear location. At least 4 cochlear samples are used at each developmental stage. Hair cell location in the cochlea was converted to frequency by the method described by Greenwood (Greenwood, 1990).

Western blots analyzing Cx26 and Cx30 protein expressions in the cochlea of cCx26 mice

Total cochlear proteins from specific regions (organ of Corti, stria vascularis and spiral ligament) were extracted using RIPA lysis buffer by following the manufacturer's instructions (Upstate Biotechnology Cell Signaling System, Lake Placid, NY). Protein concentrations were measured by using a bicinchoninic acid protein assay kit (Pierce, Rockford, IL). Proteins were separated by electrophoresis on a 12% sodium dodecyl sulphate (SDS) polyacrylamide gel. Equal amount of protein (5 μg) was loaded in each lane of the SDS gel. After transferring to nitrocellulose membrane, bands of Cx26 and Cx30 were detected on the same membrane using polyclonal antibodies against Cx26 (Invitrogen Inc., catalog# 71–0500, 0.25 μg/ml), Cx30 (Invitrogen Inc., catalog# 71–2200, 0.5 μg/ml). Details about these antibodies are given in the method section describing immuolabeling protocols. The amount of loading in each lane was further checked by Western blotting of a house-keeping protein actin (catalog# A1978, dilution factor 1:3000, Sigma-Aldrich, St. Louis, MO). Secondary antibodies used in the Western blots were goat anti-rabbit (catalog# 170–6515) and anti-mouse (catalog# 170–6516) IgG HRP conjugate (Bio-Rad Laboratories Inc., Hercules, CA). Protein bands on the blots were visualized by enhanced chemiluminescence (Super-Signal, Pierce, Rockford, IL) exposed to X-ray films (Hyper Film, Amersham Biosciences, Piscataway, NJ). Cx protein expression levels were quantified on digitized images by normalizing to the band intensity of the actin in corresponding lanes (AlphaEase software, version4.1, Alpha Innotech Corporation, Sanleandro, CA). More details of experimental procedures were given in our previous publication (Sun et al., 2005).

Results

The Cx30 null mice in the CBA/CaJ genetic background showed congenital non-syndromic deafness, a phenotype that was indistinguishable from that previously reported in other genetic backgrounds (Ahmad et al., 2007; Teubner et al., 2003). We therefore concentrated on characterizing the novel inducible cCx26 null mouse model used in this study. After giving a single injection of HTMX at E19, we found that cochleae obtained from R26R;Rosa26^{CreER} mice were positive (Fig. 1A, samples on the left) and the mice without CreER were all negative (Fig. 1A, sample on the right) for LacZ staining. Cochlear sections cut from the LacZ positive cochleae showed that the Cre recombinase activity was activated by HTMX in many cochlear cells, including patches of fibrocytes in the lateral wall and spiral limbus, cells in the stria vascularis and some SG neurons (blue staining in Fig. 1B). The regions that consistently showed the strongest LacZ staining was observed in the pillar cells and supporting cells in the organ of Corti (black arrows in Fig. 1B), which is in sharp contrast to non-homogeneous LacZ staining patterns in other regions of the cochlea. Consistent with the LacZ staining pattern shown in the R26R reporter mice, Cx26 immunoreactivity was reduced to a background level only in the organ of Corti of Cx26$^{loxP/loxP}$;Rosa26^{CreER} mice (Fig. 1, C&E, arrowhead). Since Cx26 and Cx30 are co-expressed in almost all cochlear GJs (Ahmad et al., 2003; Forge et al., 2003), co-

immunolabeling with an antibody against Cx30 on the same cochlear section was used as a control. Cx30 immunoreactivities are clearly present in the organ of Corti of cCx26 null mice, possibly forming homomeric GJs there (Fig. 1D&E, arrow and arrowhead). The non-homogeneous deletion of the *Gjb2* gene outside of the organ of Corti, as suggested by the LacZ staining patterns (Fig. 1B), was confirmed by the co-immunolabeling of whole-mount cochlear samples (Fig. 1, F&G). While Cx30 immunoreactivity showed an uninterrupted network of GJs in the membrane of all cells in the spiral limbus (red and yellow fluorescence in Fig. 1F), the Cx26 co-immunolabeled in the same region (green fluorescence in Fig. 1G) revealed the absence of Cx26 protein expression in many cells (examples are indicated by small arrows in Fig. 1G).

To quantify the change in Cx26 protein levels in various regions of the cochlea resulted from the HTMX injections in $Cx26^{loxP/loxP}$;$Rosa26^{CreER}$ mice, we performed Western blots using cochlear samples obtained separately from the stria vascularis, spiral ligament and organ of Corti (Fig. 2A). The Cx26 protein in the organ of Corti of cCx26 null mice was only 6.3±2.1% of the WT control level (n=4). Cx26 protein levels in the stria vascularis and spiral ligament were 25.7±3.8% (n=4) and 72.7±5.2% of the WT control level (n=4), respectively (Fig. 2B). Reductions in all three cochlear regions were statistically significantly ($p<0.05$). Interestingly, the protein levels of Cx30 in all three cochlear regions were unchanged from their WT control levels. They are 93.2±5.3%, 102.1±8.1% and 96.3±5.2% of the respective controls in the stria vascularis, spiral ligament and organ of Corti. The changes in Cx30 were not statistically significant ($p>0.05$) in any of the cochlear regions. These quantifications of the Cx26 and Cx30 protein levels in various cochlear regions of cCx26 null mice were consistent with the pattern suggested by immunolableing results (Fig. 1, C–G) and data obtained from the R26R;$Rosa26^{CreER}$ reporter mice (Fig. 1, A&B).

The mouse model generated by systemic HTMX injection to the $Cx26^{loxP/loxP}$;$Rosa26^{CreER}$ mice was validated further by the non-syndromic deafness displayed in all the animals (n=25) (Fig. 3). ABRs of $Cx26^{loxP/loxP}$;$Rosa26^{CreER}$ mice measured at postnatal day 21 (P21) were significantly elevated across a frequency range of 4–32 kHz (data curve linked with filled circles in Fig. 3). In contrast, the littermate-controlled pups without the $Rosa26^{CreER}$ (n=7, all received the HTMX injection at the same dosage) had normal hearing (data curve linked with filled squares in Fig. 3). The hearing loss in $Cx26^{loxP/loxP}$;$Rosa26^{CreER}$ mice gradually worsened in the next few months (Fig. 3, data curves connected by hollow circles and squares). In summary, immunolabeling data (Fig. 1 C–G), results obtained from R26R reporter mice (Fig. 1 A&B) and Western blot quantification of Cx26 protein levels (Fig. 2) all showed that a single injection of HTMX at E19 induced deletion of the *Gjb2* gene in many cochlear cells, which significantly reduced Cx26 protein level (Fig. 2) and disrupted the GJ network in the cochlea (Fig. 1F). Three independent methods consistently showed that the *Gjb2* gene was more completely deleted in the organ of Corti (Fig. 1&Fig. 2). The result that all $Cx26^{loxP/loxP}$;$Rosa26^{CreER}$ mice, but none of the $Cx26^{loxP/loxP}$ mice, displayed non-syndromic deafness (Fig. 3) after receiving HTMX injections further confirmed that we have obtained a valid mouse model for studying deafness caused by Cx26 null mutation.

We subsequently investigated the time course and pattern of cell degeneration in the cochlea of Cx30 null (Fig. 4, Fig. 5 &Fig. 7) and the cCx26 null (Fig. 6 & Fig. 7) mice. Gross morphology of the organ of Corti in the Cx30 null mice was similar to that of WT mice. The tunnel of Corti (upward arrows in Fig. 4, A–F) was opened normally in the mutant mice. No obvious atrophy of stria vascularis was observed at the resolution of optical microscopes (double arrows in Fig. 4 A&D) in Cx30 null mice, a result consistent with previous reports (Cohen-Salmon et al., 2002;Teubner et al., 2003). Even after eighteen months, the

Reissner's membrane (arrowheads, Fig. 4A&D) showed no signs of expansion or collapse, suggesting no volume change of the endolymphatic space in the Cx30 null mice. The most noticeable abnormality in the organ of Corti was the loss of outer HCs. Enlarged views of the organ of Corti obtained from the mutant mice are shown in Fig. 4 B&C, and E&F. Missing OHCs in cochlear sections are indicated by arrowheads in these panels, which showed a gradually worsening of the degeneration of OHCs (comparing Fig. 4 B&C to E&F). Although the exact time course of the HC death in the Cx30 null mice was variable in individual animals, most OHCs in all cochlear turns were degenerated 6 month after birth. In contrast, degeneration of inner HCs in the Cx30 mice was much slower. A loss of inner HCs was observed initially at about P21 in the basal turn. However, most inner HCs in the apical (slanted small arrows in Fig. 4 B&E) and middle (slanted small arrows in Fig. 4 C&F) turns survived for up to 18 months. Details of the pattern and time course of HC degeneration are given in Fig. 7. Another common finding in all the cochlear turns of Cx30 null mice was that the supporting cells survived for a long period of time after the death of outer HCs (Fig. 4 B–F). The normal tunnel of Corti in all cochlear sections (upward arrows in Fig. 4) suggested survival of both inner and outer pillar cells during the one and a half year period. Another interesting observation is that the supporting cells did not appear to grow into the empty space created by degenerated OHCs (Fig. 4 B–F). For comparison, morphology of the organ of Corti obtained from WT mice at one (Fig. 4G) and eighteen (Fig. 4H) months are given.

Long-term survival of most SG neurons in the cochlea of Cx30 null mice was generally observed (animal number (n) is greater than 6 in all cases). Cochlear sections obtained from WT (panels A–I in Fig. 5) and Cx30 null (panels a–i in Fig. 5) mice cut from one-month, six-month and eighteen-month old animals were compared. Apical, middle and basal turns are shown in the top, middle and bottom rows, respectively (picture panels on top of Fig. 5). Loss of SG neurons in the basal turn during the 18 month period was never statistically significant (Fig. 5J, triangles connected by a dotted line). Degeneration of SG neurons in the middle and apical turns became statistically significant only after 12 and 6 months of deafness (data points marked by asterisks in Fig. 5J), respectively. Most SG neurons in all cochlear turns survived after 18 months of deafness in the Cx30 null mice with a CBA/CaJ genetic background. The apical turn of the cochlea showed the most severe degeneration of SG neurons, a little more than half (54.6±2.7%) of neurons survived after 18 months of deafness (Fig. 5J, squares connected by a solid line). Soma of survived SG neurons sometimes clustered together to form isolated islands in the spiral ganglia. One example is indicated by an arrow in Fig. 5 g.

Similar to Cx30 null mice, gross cochlear morphology of cCx26 null mice was similar to that of the WT mice (Fig. 6, A&C). The Reissner's membrane was relatively straight (Fig. 6C), indicating that the volume of the endolymphatic space was not significantly changed. No obvious atrophy of stria vascularis was observed at the optical microscope level (small arrow in Fig. 6C), although further investigations at the electron microscope level are certainly needed to fully address this issue. In comparison to the Cx30 null mice, cellular degeneration in the organ of Corti and SG in the cCx26 null mice was considerably more severe and rapid. One month after deafness, most SG neurons in the middle turn were already degenerated, while neurons in the apical and basal turns of the same cochlea were relatively intact (Fig. 6A&F). Three month after birth, most SG neurons in both middle and basal turns were lost, while a majority of SG neurons in the apical turn were still present (Fig. 6B&F). By five months, almost all SG neurons in the middle (Fig. 6D&F) and basal (Fig. 6E&F) turns were disappeared. Significant amounts of SG neurons in the apical turn, however, are not degenerated. Fig. 6C shows one examples in which many survived SG neurons were clustered together (indicated by a white arrow in Fig. 6C) in the spiral ganglia. Judging by morphological criteria, only about one quarter of the soma of SG neurons

(26.8±6.2% of WT control, n=8) survived at P30 in the middle turn cochlea (Fig. 6F, solid circles connected by a dashed line). Most SG neurons in the middle and basal cochlear turns of cCx26 mice died 3 months after birth (Fig. 6B&F). Quantification showed that the degeneration progressed even further at 5 months (Fig. 6F, solid circles and triangles). In comparison, degeneration of SG neurons in the apical turn (Fig. 6, A–C) was relatively mild. Most SG neurons (68.3±6.2%, n=8) in the apical turn survived at the end of 5 months (solid squares connected by a solid line), the longest time observed in this project for cCx26 null mice.

In the organ of Corti of cCx26 null mice, first groups of degenerated cells were found around P14 in the middle turn outer HCs and the supporting cells surrounding outer HCs (indicated by double arrows in Fig. 6G). Strikingly, the inner HCs in the same cochlear location were clearly present (indicated by a single arrow in Fig. 6G). Cell death in the organ of Corti quickly spread from middle turn to the basal turns. All types of cells in the middle and basal turn organ of Corti were disappeared in cCx26 null mice a few months after birth (upward arrowheads in Fig. 6D&E). Peripheral nerve fibers and soma of the SG neurons at corresponding cochlear locations were completely degenerated as well. Surpringly, HCs in the apical turn of cCx26 null mice were relatively intact. One row of inner HC and three rows of OHCs are clearly distinguishable in a cochlear section obtained from a five month old apical cochlea of cCx26 null mouse (Fig. 6H), although .

To better quantify the loss of hair cells in the cochlea of Cx mutant mice, we obtained cochleograms from age-matched WT and mutant mice. Picture panels in figure7 give examples of hair cell nuclei (examples are indicated by white arrows in Fig. 7A) obtained from small segments of the organ of Corti from WT (Fig. 7, A–I & K–P), Cx30 null (Fig. 7, a–i) and cCx26 null (Fig. 7, k–p) mice. Counts of cell nuclei were compared between the WT and the Cx30 null mice to obtain percentage of OHC loss at particular cochlear locations at various developmental time points from P18 to P18 months (Fig. 7J). Loss of OHCs at high-frequency regions of Cx30 null mice was evident at P18. Over a time period of 18 months it gradually expanded to the low frequency regions (Fig. 7 a–i and Fig. 7J). In contrast, inner HCs were relatively intact in Cx30 null mice (Fig.7, comparing G–I with g–i). At the end of 18 months the percentage of inner HC loss was 52.2±9.6%, 28.7±8.9% and 10.5±3.8% at basal, middle and apical turns, respectively.

In cCx26 null mice, HC degeneration in the cochlea started in the middle turn and followed a more rapid time course and a pattern that is distinctively different from that of Cx30 null mice. Most inner and outer HCs were lost one month after birth in the middle turn (Fig. 7i), while HCs in the apical (Fig. 7k) and basal (Fig. 7m) turns were relatively intact (Fig. 7Q). In a time course of about 3 months, most HCs in the basal turn were also dead (Fig. 7p and Fig. 7Q). Only the nuclei of inner and outer HCs at the apical turn were still visible (Fig. 7n).

In summary, dramatically different time courses of cell death were found in the cochlea of Cx30 null and cCx26 null mice. The HC death and secondary degeneration of SG neurons in the cochlea of cCx26 null mice were dramatically more widespread and rapid than those observed in the Cx30 null mice.

Discussion

Since previous studies indicated that most GJs in the cochlea are co-assembled from Cx26 and Cx30 (Forge et al., 2003; Sun et al., 2005), we expected that genetic deletion of either one of them should generate similar pathological patterns in the cochlea. Using a previously-validated Cx30 null (Teubner et al., 2003) and a novel inducible cCx26 null mouse models,

however, we found a surprisingly different time course and pattern of cellular degeneration in the cochlea of the two mutant mouse models. Comparing to dramatically rapid degeneration of both HCs and SG neurons in the cCx26 mice, cell death in the cochlea of Cx30 null mice was relatively mild and slow. Many supporting cells and inner HCs in the organ of Corti of the Cx30 null mice survived even after 18 months of deafness (Fig. 4). Within one month, all types of cells in the middle turn organ of Corti (including inner and outer HCs, all types of cochlear supporting cells) of cCx26 null mice disintegrated (Fig. 6). Our results (Fig. 6&Fig. 7) clearly demonstrated that cell death in the organ of Corti started in the middle turn of the cochlea. This region covers a frequency range of 8k-20k Hz (Fig. 7Q), which is the most sensitive for the hearing of mice. Considering that cell death in the organ of Corti of cCx26 null mice didn't happen until after the onset of hearing at around P12, it is possible that the cell death is coupled with sound-driven activities in the organ of Corti. This could provide one theory explaining why the most sensitive region along the basilar membrane (8–20kHz) displayed most severe degeneration. These sharp contrasts provide the first indication that heterogeneous mechanisms may be responsible for deafness caused by Cx26 and Cx30 null mutations. In addition, this study provides the first investigation of secondary degeneration of SG neurons due to genetic mutations of the genes coding for Cx26 and Cx30. In the past, the time course and pattern of cellular degeneration in the cochlea resulting from exposure to loud noise (Bohne and Harding, 2000; Liberman and Kiang, 1978), or aminoglycoside (Koitchev et al., 1982; Leake and Hradek, 1988; McFadden et al., 2004), or chemotherapeutic ototoxic drugs (Wang et al., 2003) have been investigated extensively.

Important differences in cochlear pathology exist between the current and a previously-reported cCx26 mouse models (Cohen-Salmon et al., 2002). The rapid death of cells in the cochlear sensory epithelium and SG neurons was not observed in the previously-reported cCx26 null mouse model (Cohen-Salmon et al., 2002). We observed that the earliest cell death started in OHCs and the supporting cells surrounding the OHCs (Fig. 6G), while Cohen-Salmon et al. noted that supporting cells around the inner HCs were the first groups of cells to degenerate. The reason for these discrepancies certainly warrants more investigations. While the previous cCx26 null mice were generated by a spatially-specific approach that targeted the deletion of the *Gjb2* in the cochlear sensory epithelium (Cohen-Salmon et al., 2002), we created the cCx26 null mice in this study with a time-specific method which may produce a more widespread disruption of GJ network in the cochlea. The more extensive damage to the GJ-mediated functions may involve the glucose transportation to avascular sensory epithelium of the cochlea (Chang et al., 2008). A severe reduction in glucose supply caused by the absence of Cx26 during the cochlear development is a novel hypothesis currently being tested in our laboratory for the cellular degenerations observed in the new cCx26 null mouse model reported here. Alternatively, disruption of the GJ hemichannel functions during cochlear development (Anselmi et al., 2008; Zhao et al., 2005) may also severely damage the homeostasis in the cochlea that ultimately result in cell death in the organ of Corti.

Most cases of sensorineural hearing loss are caused by loss of HCs in the cochlea (Hudspeth, 2000). The HCs are a major source of neurotrophic support for the SG neurons (Ylikoski et al., 1993). HC loss induces degeneration of SG neurons in cochlear regions that corresponds to the location of the HC damage caused by loud noises (Johnsson, 1974; Sugawara et al., 2005). In contrast, substantial loss of SG neurons does not seem to result in significant death of HCs in the organ of Corti (Schmiedt et al., 2002; Sugawara et al., 2005). These results indicate that HC survival does not require the innervation of nerve terminals, whereas death of cells in the sensory epithelium triggers secondary degeneration of SG neurons. There were a large number of residual inner HCs and supporting cells in the organ of Corti of Cx30 null mice, even after 18 months of deafness (Fig. 4). In contrast, cell death

in the organ of Corti of cCx26 mice included both inner HCs and supporting cells (Fig. 6). These results are consistent with previous studies showing that the survival of inner HCs and supporting cells is vital for maintaining viable SG neurons. A small percentage of remaining inner HCs can support the survival of a much larger percentage of SG neurons in regions where supporting cells remain (Johnsson, 1974; McFadden et al., 2004; Sugawara et al., 2005). Long-term survival of SG neurons without the presence of inner HCs are also reported (Sugawara et al., 2005), provided that the supporting cells are present. It seems reasonable to speculate that both inner HCs and supporting cells release neurotrophins that protect SG neurons from degeneration, thus explaining the exceptional amounts of surviving SG neurons in the cochlea of Cx30 null mice.

The degeneration time course of SG neurons ranges from a few weeks to years, depending on the species (Jyung et al., 1989; Leake and Hradek, 1988; Otte et al., 1978). The loss of HCs results in >80% loss of SG neurons in a few weeks in mice, rats, cats and guinea pigs deafened by ototoxic drugs (Dodson and Mohuiddin, 2000; Hardie and Shepherd, 1999; Leake and Hradek, 1988), although the secondary degeneration of SG neurons in humans appear to be much slower (Linthicum et al., 1991). The substantial loss of SG neurons below a critical level is likely to reduce the benefits of the cochlear implant, which could result in poor performance in patients (Clopton et al., 1980; Incesulu and Nadol, 1998; Skinner et al., 2002). The degeneration of significant amounts of SG neurons also diminishes the hope for developing future treatments that are based on the regeneration of hair cells. Thus, preventing the loss of SG neurons may considerably enhance the benefits of the cochlear implant, which may lead to better language acquisition and speech perception for at least a significant subset of patients. The precise pattern of SG neuron survival in human patients suffering various kinds of Cx26 and Cx30 loss-of-function mutations is unknown. If we extrapolate the data obtained from current animal studies, the results suggest that optimal placement for the electrode of cochlear implants may be different for patients suffering from Cx26 and Cx30 null mutations.

Acknowledgments

This study was supported by grants to X. Lin from NIDCD (RO1-DC006483 and R21-DC008353), National Natural Science Foundation (30728029) of China and the Woodruff Foundation. W. Tang received grants from NIDCD (R21 DC008672) and the Deafness Research Foundation. Y. Sun and Y. Wang were partially supported by grants from China Scholarship Council (grant#:200710187 and 2008610021).

Other Acknowledgement

We thank Mrs. Binfei Zhou for excellent technical support in mouse breeding and genotyping, and Dr. Ping Chen at the Department Cell Biology, Emory University School of Medicine for providing the R26R reporter mice used in the studies. The authors are grateful for Miss Anne Lin for proofreading the manuscript.

Source of funding: National Institute of Deafness and other Communicative Disorders

Literature Cited

Ahmad S, Chen S, Sun J, Lin X. Connexins 26 and 30 are co-assembled to form gap junctions in the cochlea of mice. Biochem Biophys Res Commun. 2003; 307(2):362–368. [PubMed: 12859965]

Ahmad S, Tang W, Chang Q, Qu Y, Hibshman J, Li Y, Sohl G, Willecke K, Chen P, Lin X. Restoration of connexin26 protein level in the cochlea completely rescues hearing in a mouse model of human connexin30-linked deafness. Proceedings of the National Academy of Sciences of the United States of America. 2007; 104(4):1337–1341. [PubMed: 17227867]

Anselmi F, Hernandez VH, Crispino G, Seydel A, Ortolano S, Roper SD, Kessaris N, Richardson W, Rickheit G, Filippov MA, Monyer H, Mammano F. ATP release through connexin hemichannels and gap junction transfer of second messengers propagate Ca2+ signals across the inner ear.

Proceedings of the National Academy of Sciences of the United States of America. 2008; 105(48): 18770–18775. [PubMed: 19047635]

Bohne BA, Harding GW. Degeneration in the cochlea after noise damage: primary versus secondary events. Am J Otol. 2000; 21(4):505–509. [PubMed: 10912695]

Chang EH, Van Camp G, Smith RJ. The role of connexins in human disease. Ear Hear. 2003; 24(4): 314–323. [PubMed: 12923422]

Chang Q, Tang W, Ahmad S, Zhou B, Lin X. Gap junction mediated intercellular metabolite transfer in the cochlea is compromised in connexin30 null mice. PLoS ONE. 2008; 3(12):e4088. [PubMed: 19116647]

Clopton BM, Spelman FA, Miller JM. Estimates of essential neural elements for stimulation through a cochlear prosthesis. Ann Otol Rhinol Laryngol. 1980; Suppl 89(2 Pt 2):5–7.

Cohen-Salmon M, Ott T, Michel V, Hardelin JP, Perfettini I, Eybalin M, Wu T, Marcus DC, Wangemann P, Willecke K, Petit C. Targeted ablation of connexin26 in the inner ear epithelial gap junction network causes hearing impairment and cell death. Curr Biol. 2002; 12(13):1106–1111. [PubMed: 12121617]

Cullen RD, Buchman CA, Brown CJ, Copeland BJ, Zdanski C, Pillsbury HC 3rd, Shores CG. Cochlear implantation for children with GJB2-related deafness. Laryngoscope. 2004; 114(8):1415–1419. [PubMed: 15280719]

Denoyelle F, Weil D, Maw MA, Wilcox SA, Lench NJ, Allen-Powell DR, Osborn AH, Dahl HH, Middleton A, Houseman MJ, Dode C, Marlin S, Boulila-ElGaied A, Grati M, Ayadi H, BenArab S, Bitoun P, Lina-Granade G, Godet J, Mustapha M, Loiselet J, El-Zir E, Aubois A, Joannard A, Petit C, et al. Prelingual deafness: high prevalence of a 30delG mutation in the connexin 26 gene. Human molecular genetics. 1997; 6(12):2173–2177. [PubMed: 9336442]

Dodson HC, Mohuiddin A. Response of spiral ganglion neurones to cochlear hair cell destruction in the guinea pig. J Neurocytol. 2000; 29(7):525–537. [PubMed: 11279367]

Ernfors P, Van De Water T, Loring J, Jaenisch R. Complementary roles of BDNF and NT-3 in vestibular and auditory development. Neuron. 1995; 14(6):1153–1164. [PubMed: 7605630]

Forge A, Becker D, Casalotti S, Edwards J, Marziano N, Nevill G. Gap junctions in the inner ear: comparison of distribution patterns in different vertebrates and assessement of connexin composition in mammals. J Comp Neurol. 2003; 467(2):207–231. [PubMed: 14595769]

Gabriel HD, Jung D, Butzler C, Temme A, Traub O, Winterhager E, Willecke K. Transplacental uptake of glucose is decreased in embryonic lethal connexin26-deficient mice. J Cell Biol. 1998; 140(6):1453–1461. [PubMed: 9508777]

Greenwood DD. A cochlear frequency-position function for several species--29 years later. J Acoust Soc Am. 1990; 87(6):2592–2605. [PubMed: 2373794]

Grifa A, Wagner CA, D'Ambrosio L, Melchionda S, Bernardi F, Lopez-Bigas N, Rabionet R, Arbones M, Monica MD, Estivill X, Zelante L, Lang F, Gasparini P. Mutations in GJB6 cause nonsyndromic autosomal dominant deafness at DFNA3 locus. Nature genetics. 1999; 23(1):16–18. [PubMed: 10471490]

Guillery RW. On counting and counting errors. J Comp Neurol. 2002; 447(1):1–7. [PubMed: 11967890]

Hardie NA, Shepherd RK. Sensorineural hearing loss during development: morphological and physiological response of the cochlea and auditory brainstem. Hear Res. 1999; 128(1–2):147–165. [PubMed: 10082295]

Hudspeth AJ. Hearing and deafness. Neurobiol Dis. 2000; 7(5):511–514. [PubMed: 11042065]

Incesulu A, Nadol JB Jr. Correlation of acoustic threshold measures and spiral ganglion cell survival in severe to profound sensorineural hearing loss: implications for cochlear implantation. Ann Otol Rhinol Laryngol. 1998; 107(11 Pt 1):906–911. [PubMed: 9823838]

Johnsson LG. Sequence of degeneration of Corti's organ and its first-order neurons. Ann Otol Rhinol Laryngol. 1974; 83(3):294–303. [PubMed: 4829736]

Jyung RW, Miller JM, Cannon SC. Evaluation of eighth nerve integrity by the electrically evoked middle latency response. Otolaryngol Head Neck Surg. 1989; 101(6):670–682. [PubMed: 2512556]

Kelsell DP, Dunlop J, Stevens HP, Lench NJ, Liang JN, Parry G, Mueller RF, Leigh IM. Connexin 26 mutations in hereditary non-syndromic sensorineural deafness. Nature. 1997; 387(6628):80–83. [PubMed: 9139825]

Koitchev K, Guilhaume A, Cazals Y, Aran JM. Spiral ganglion changes after massive aminoglycoside treatment in the guinea pig. Counts and ultrastructure. Acta Otolaryngol. 1982; 94(5–6):431–438. [PubMed: 6184939]

Leake PA, Hradek GT. Cochlear pathology of long term neomycin induced deafness in cats. Hear Res. 1988; 33(1):11–33. [PubMed: 3372368]

Liberman MC, Kiang NY. Acoustic trauma in cats. Cochlear pathology and auditory-nerve activity. Acta Otolaryngol. 1978 Suppl 358:1–63.

Linthicum FH Jr, Fayad J, Otto SR, Galey FR, House WF. Cochlear implant histopathology. American Journal of Otology. 1991; 12(4):245–311. [PubMed: 1928309]

McFadden SL, Ding D, Jiang H, Salvi RJ. Time course of efferent fiber and spiral ganglion cell degeneration following complete hair cell loss in the chinchilla. Brain Res. 2004; 997(1):40–51. [PubMed: 14715148]

Otte J, Schunknecht HF, Kerr AG. Ganglion cell populations in normal and pathological human cochleae. Implications for cochlear implantation. Laryngoscope. 1978; 88(8 Pt 1):1231–1246. [PubMed: 672357]

Schecterson LC, Bothwell M. Neurotrophin and neurotrophin receptor mRNA expression in developing inner ear. Hearing Research. 1994; 73(1):92–100. [PubMed: 8157510]

Schmiedt RA, Okamura HO, Lang H, Schulte BA. Ouabain application to the round window of the gerbil cochlea: a model of auditory neuropathy and apoptosis. J Assoc Res Otolaryngol. 2002; 3(3):223–233. [PubMed: 12382099]

Skinner MW, Holden LK, Holden TA, Demorest ME, Fourakis MS. Speech recognition at simulated soft, conversational, and raised-to-loud vocal efforts by adults with cochlear implants. J Acoust Soc Am. 1997; 101(6):3766–3782. [PubMed: 9193063]

Skinner MW, Ketten DR, Holden LK, Harding GW, Smith PG, Gates GA, Neely JG, Kletzker GR, Brunsden B, Blocker B. CT-derived estimation of cochlear morphology and electrode array position in relation to word recognition in Nucleus-22 recipients. J Assoc Res Otolaryngol. 2002; 3(3):332–350. [PubMed: 12382107]

Soriano P. Generalized lacZ expression with the ROSA26 Cre reporter strain. Nature genetics. 1999; 21(1):70–71. [PubMed: 9916792]

Sugawara M, Corfas G, Liberman MC. Influence of supporting cells on neuronal degeneration after hair cell loss. J Assoc Res Otolaryngol. 2005; 6(2):136–147. [PubMed: 15952050]

Sun J, Ahmad S, Chen S, Tang W, Zhang Y, Chen P, Lin X. Cochlear gap junctions coassembled from Cx26 and 30 show faster intercellular Ca2+ signaling than homomeric counterparts. Am J Physiol Cell Physiol. 2005; 288(3):C613–C623. [PubMed: 15692151]

Teubner B, Michel V, Pesch J, Lautermann J, Cohen-Salmon M, Sohl G, Jahnke K, Winterhager E, Herberhold C, Hardelin JP, Petit C, Willecke K. Connexin30 (Gjb6)-deficiency causes severe hearing impairment and lack of endocochlear potential. Human molecular genetics. 2003; 12(1): 13–21. [PubMed: 12490528]

Vooijs M, Jonkers J, Berns A. A highly efficient ligand-regulated Cre recombinase mouse line shows that LoxP recombination is position dependent. EMBO Rep. 2001; 2(4):292–297. [PubMed: 11306549]

Waltzman SB, Cohen NL, Gomolin RH, Green JE, Shapiro WH, Hoffman RA, Roland JT Jr. Open-set speech perception in congenitally deaf children using cochlear implants. Am J Otol. 1997; 18(3): 342–349. [PubMed: 9149829]

Wang J, Ding D, Salvi RJ. Carboplatin-induced early cochlear lesion in chinchillas. Hear Res. 2003; 181(1–2):65–72. [PubMed: 12855364]

Willecke K, Eiberger J, Degen J, Eckardt D, Romualdi A, Guldenagel M, Deutsch U, Sohl G. Structural and functional diversity of connexin genes in the mouse and human genome. Biol Chem. 2002; 383(5):725–737. [PubMed: 12108537]

Ylikoski J, Pirvola U, Moshnyakov M, Palgi J, Arumae U, Saarma M. Expression patterns of neurotrophin and their receptor mRNAs in the rat inner ear. Hearing Research. 1993; 65(1–2):69–78. [PubMed: 8080462]

Zhao HB, Yu N, Fleming CR. Gap junctional hemichannel-mediated ATP release and hearing controls in the inner ear. Proceedings of the National Academy of Sciences of the United States of America. 2005; 102(51):18724–18729. [PubMed: 16344488]

Zheng QY, Johnson KR, Erway LC. Assessment of hearing in 80 inbred strains of mice by ABR threshold analyses. Hear Res. 1999; 130(1–2):94–107. [PubMed: 10320101]

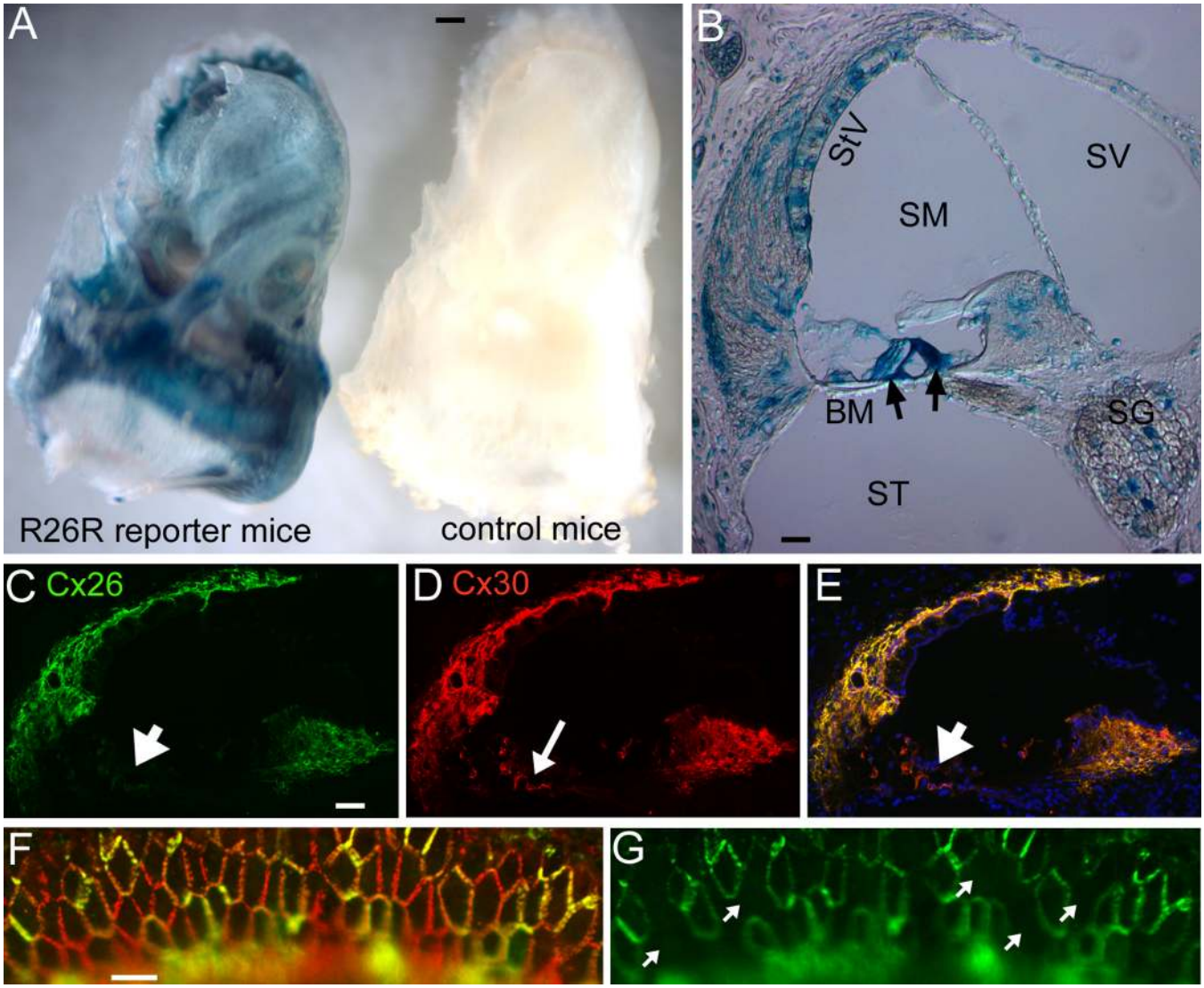

Figure 1. Summary of data validating the cCx26 null mouse model used in the study (a magenta-green version of this figure is given as a supplemental figure)

(A): Comparison of two cochleae obtained from R26R mice with (left) or without (right) the Cre-ER. Mice were injected with HTMX at E19 and the Cre recombinase activities were visualized by the blue LacZ staining.

(B): A cochlear section cut from a R26R;R26cre-ER^{T} reporter mouse received injection of HTMX. Pattern of Cre recombinase activation was visualized by LacZ staining. Landmark structures of the cochlea are labeled. StV: stria vascularis; SM: scala media; SV: scala vestibuli; BM: basilar membrane; ST: scala tympani; SG: spiral ganglia.

(C)–(E): Co-immunolabeling of Cx26 (C) and Cx30 (D) in cochlear cyrosections of Cx26$^{loxP/loxP}$;Rosa26^{CreER} mice after they were injected with HTMX at E19. (E) is the overlapped images of (C) and (D). Fluorescent image of DAPI staining on the same cochlear section is also superimposed.

(F): Co-immunolabeling of Cx26 (green) and Cx30 (red) obtained from spiral limbus region of a whole-mount cochlear preparation of a Cx26$^{loxP/loxP}$;Rosa26^{CreER} mouse after HTMX injection. For clarity, the green channel image for Cx26 immunolabeling is given again in (G). Arrows point to examples of cells that are not expressing Cx26.

Scale bars are approximately 250 μm for panel A and 100 μm for other panels.

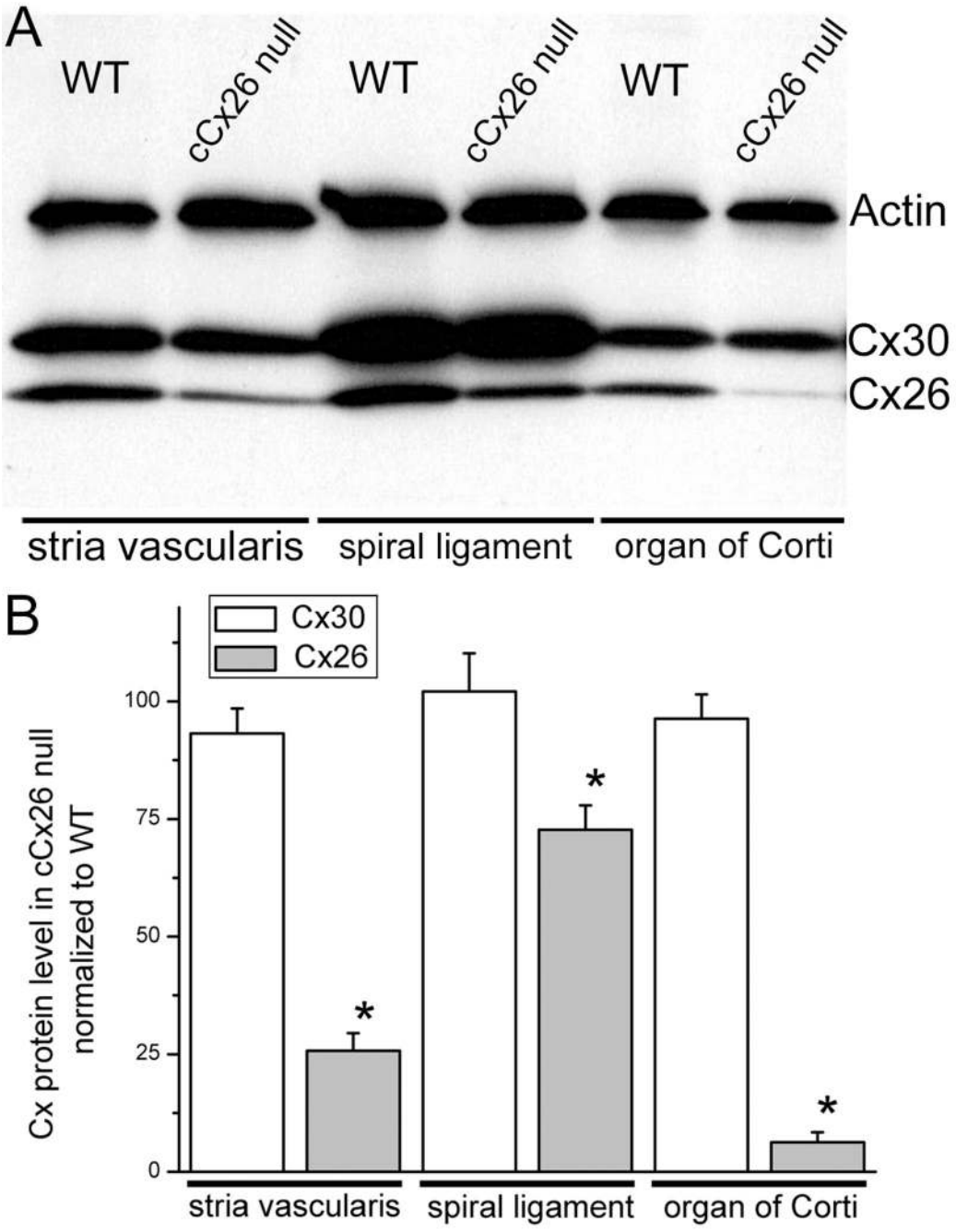

Figure 2. Protein levels of Cx26 and Cx30 in three different regions of the cochlea of cCx26 null and WT control mice

(A) Western blots measuring Cx26 and Cx30 in stria vascularis, spiral ligament and organ of Corti of WT and cCx26 null mice. Legends for each lane are given in the figure. The band intensities are normalized to the corresponding actin bands for quantification (B). Asterisks on top of bars indicate significant reduction in Cx26 protein expression compared with the WT controls in that specific cochlear region.

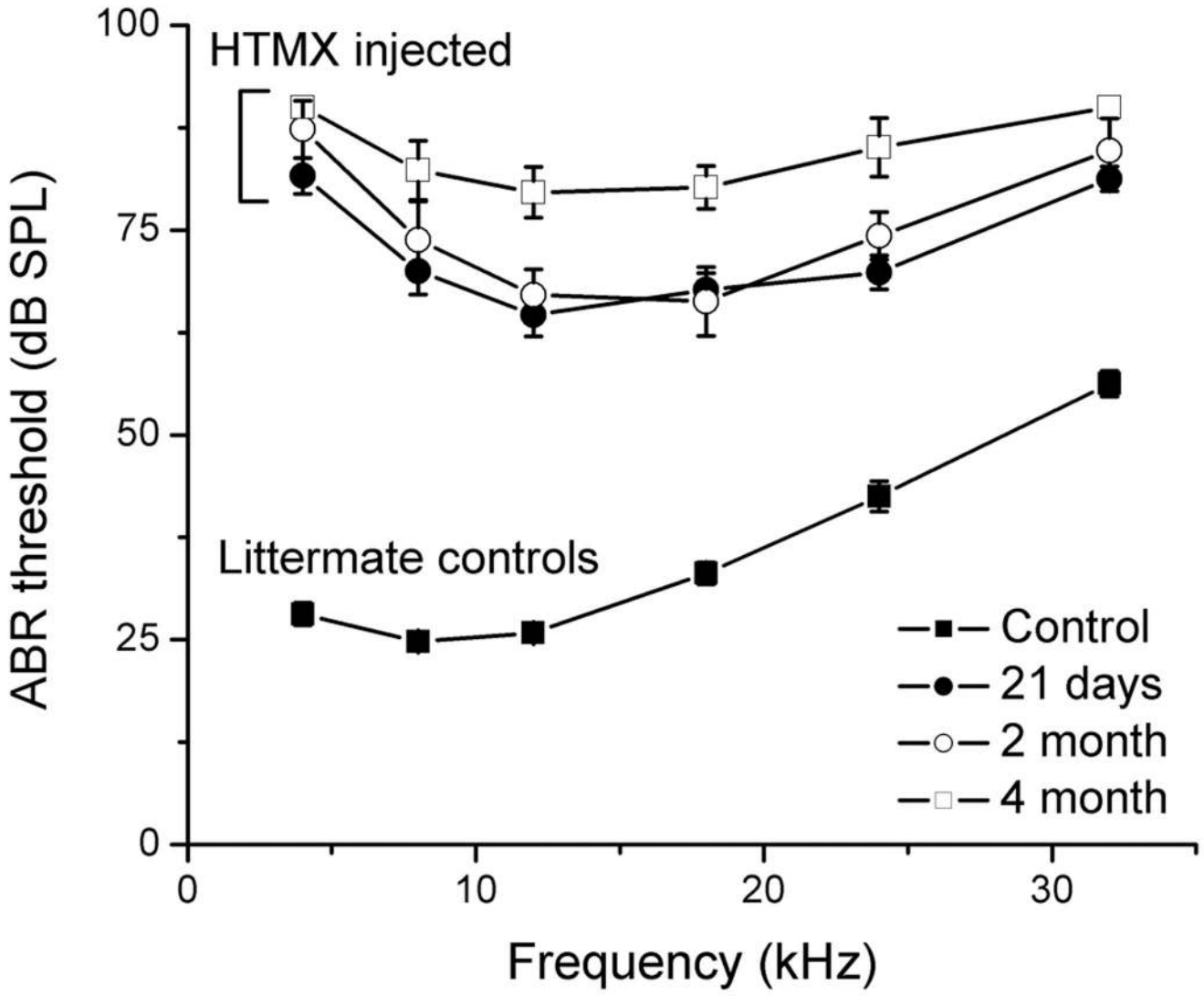

Figure 3. Hearing thresholds (y-axis) determined by ABR measurements at various frequencies (x-axis) for cCx26 null mice and littermate-control mice

ABR thresholds were measured at postnatal day 21 (P21), 2 and 4 months from cCx26 null mice generated by HTMX injection. Legends for symbols and lines are given in the figure. Vertical bars represent standard errors of the mean.

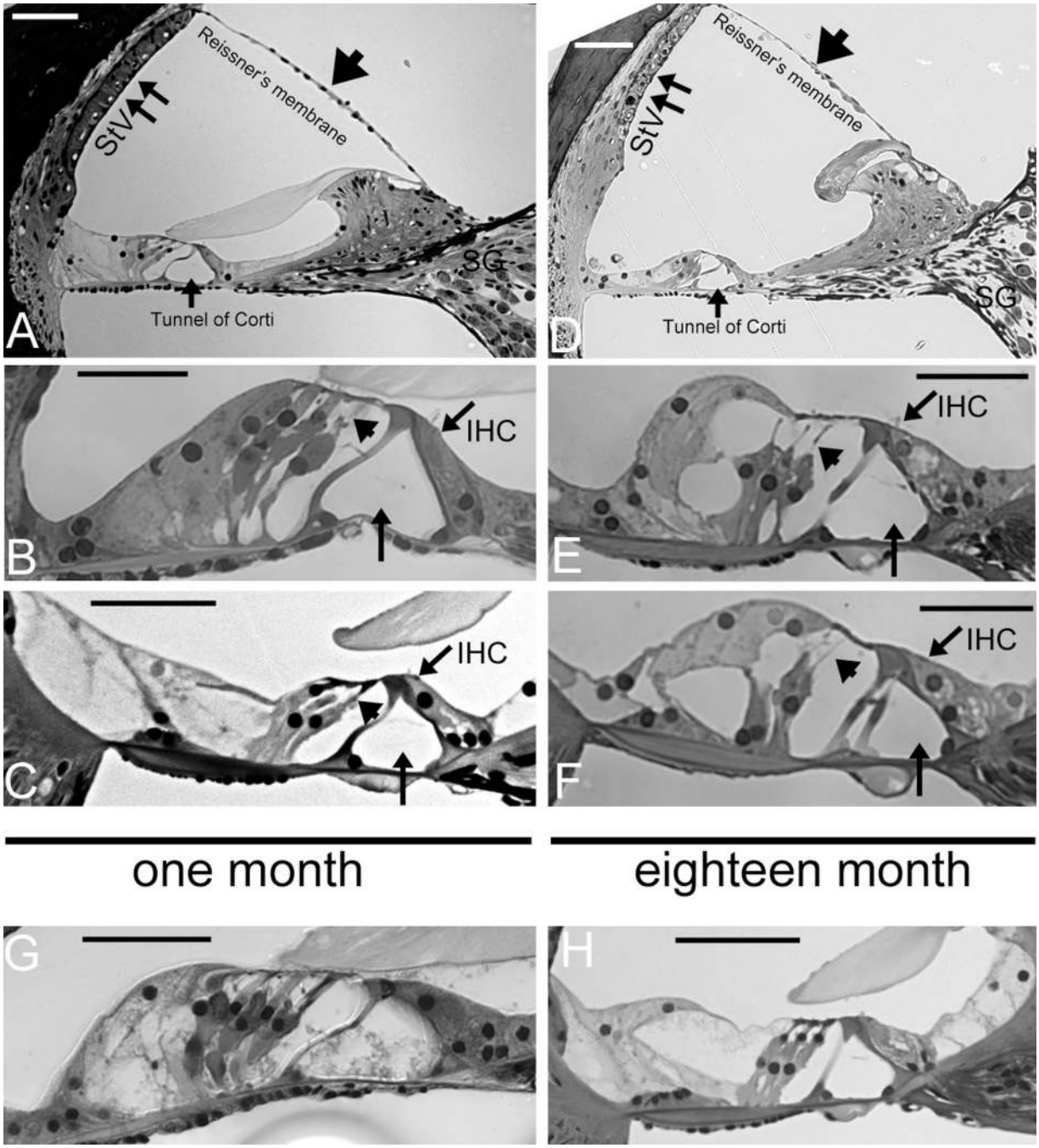

Figure 4. Gross cochlear morphology and patterns of cell death in the organ of Corti of Cx30 null mice observed at one (panels on the left column) and eighteen (panels on the right column) months

Cochlear sections of Cx30 null mice showing the gross morphology of an entire cochlear turns observed at one (A) and eighteen (D) months after birth. (B) and (C) are enlarged views showing apical and middle turn organ of Corti observed at one month. (E) and (F) are apical and middle organ of Corti observed at eighteen months. For comparison, (G) and (H) show the morphology of the organ of Corti obtained from WT mice at one and eighteen months, respectively. Scale bars represent approximately 100 μm.

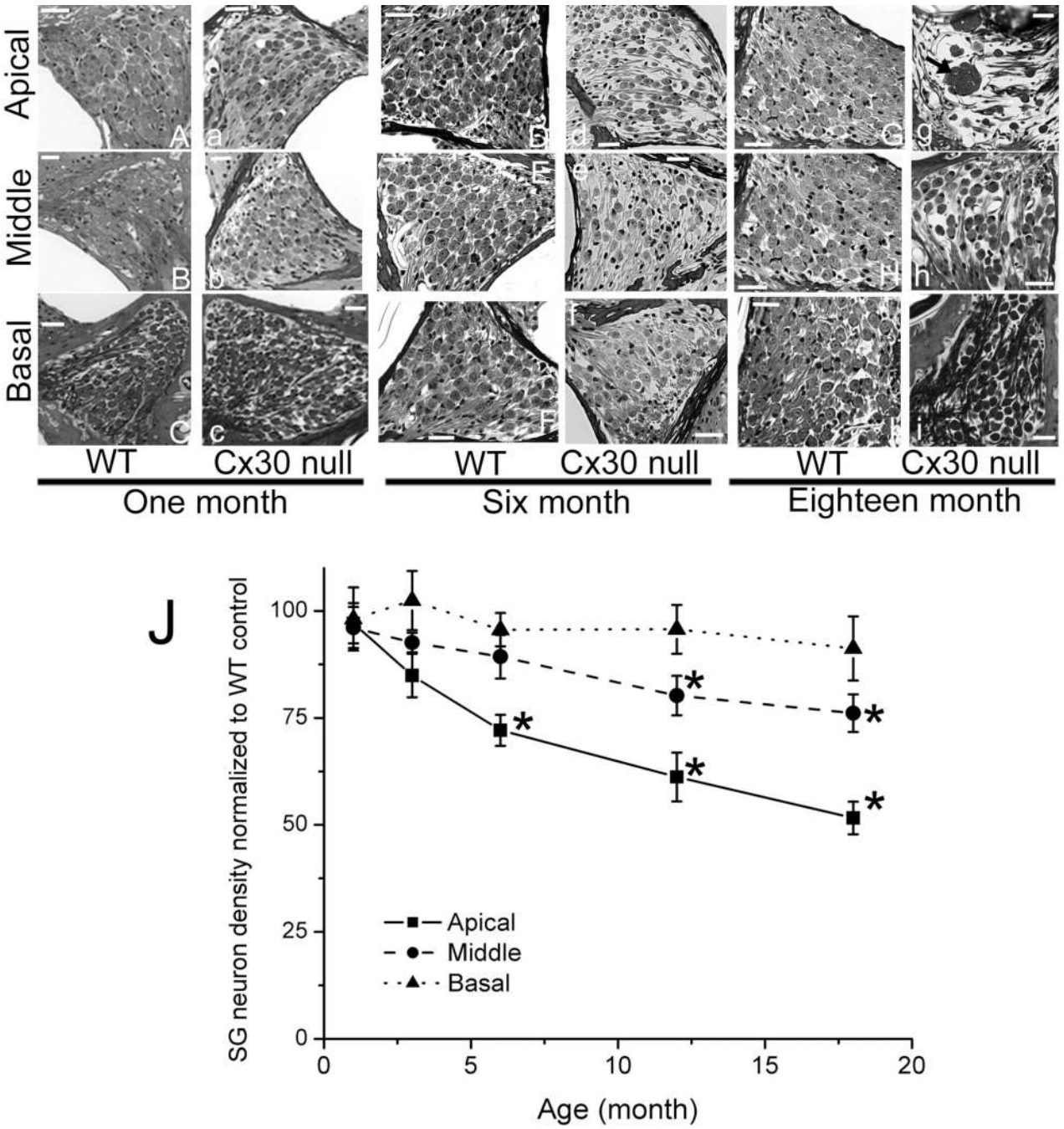

Figure 5. Survival of SG neurons in Cx30 null mice at various time points (1–18 months) after birth

Picture panels show examples of SG neurons of WT (A–I) and age-matched Cx30 null (a–i) mice. J) Relative survival of SG neurons (y-axis) in Cx30 null mice at various time points after birth (x-axis) was obtained by normalizing to age-matched WT samples. Asterisks denote data points when statistically significant reduction in SG neuron density are shown ($p<0.05$). Legends for symbols and lines are given in the figure.

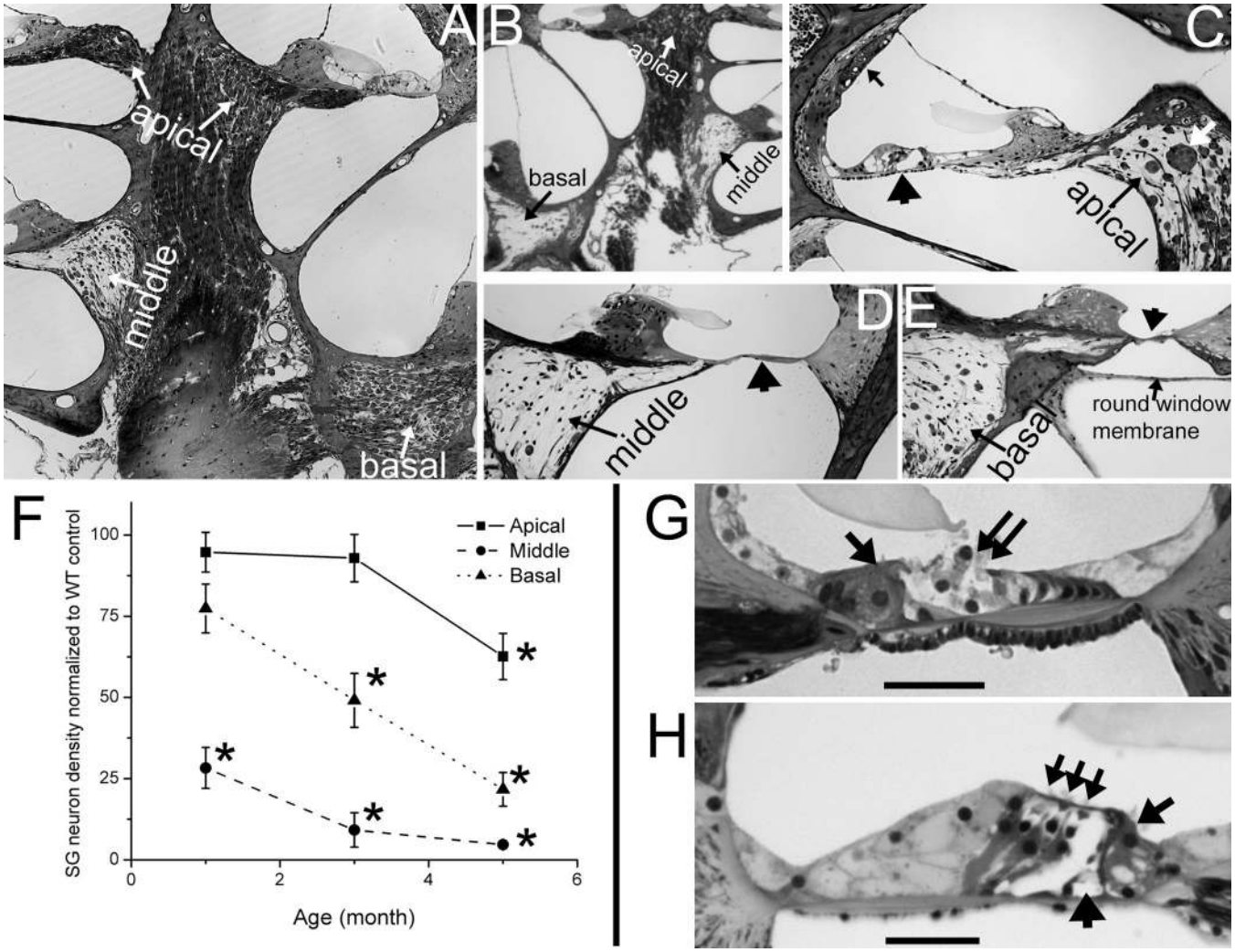

Figure 6. Pattern and time course of cell degeneration in the cochlea of cCx26 null mice

(A) Modiolus of a cochlea obtained from a one-month old cCx26 null mouse comparing the degeneration of SG neurons in the apical, middle and basal turns. (B) Modiolus of a cochlea obtained from a three-month old cCx26 null mouse comparing the degeneration of SG neurons in the apical, middle and basal turns. (C–E) Spiral ganglia of apical (C), middle (D) and basal (E) turn obtained from a five-month old cCx26 null mouse. (F) Relative survival of SG neurons (normalized to age-matched WT controls, y-axis) in cCx26 null mice at various time points after birth (x-axis). Asterisks denote data points when statistically significant reduction from WT controls are shown ($p<0.05$). Legends for symbols and lines are given in the figure. (G) Morphology of the organ of Corti observed from the middle turn cochlea of a P14 cCx26 null mouse. (H) Apical organ of Corti obtained from the cochlea of a five-month old cCx26 null mouse. Scale bars represent approximately 100 μm.

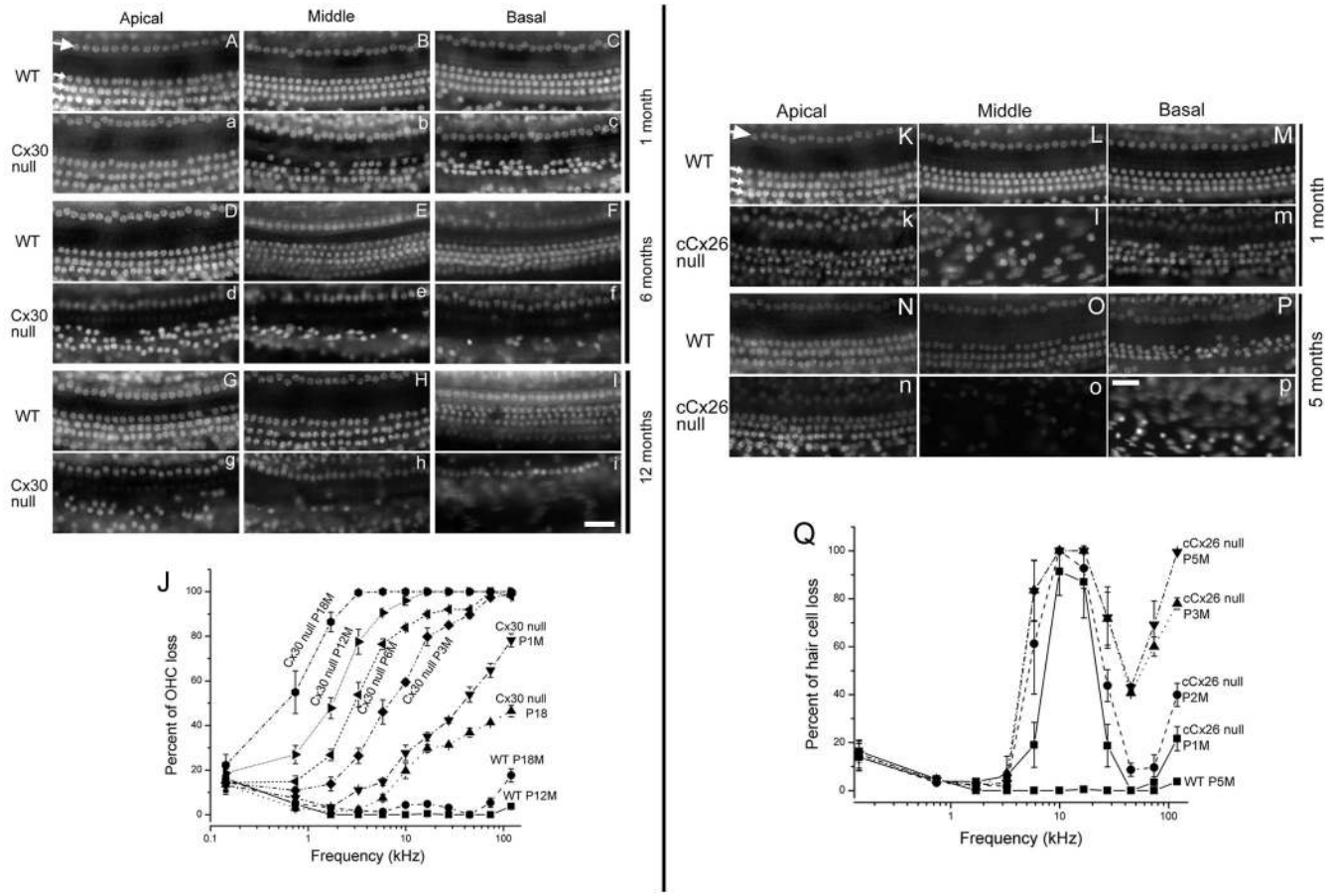

Figure 7. Pattern and time course of HC death in Cx30 null (panels on the left) and cCx26 null (panels on the right) mice

Picture panels give examples HC nuclei stained with DAPI from WT (A-I for Cx30 null control, K–P for cCx26 null control), Cx30 null (a–i) and cCx26 null (k–p) mice. Quantifications of HC loss (normalized to age-matched WT controls) at specific cochlear locations (cochleograms) for Cx30 null (J) and cCx26 null (Q) are given. Legends for symbols and lines in the picture are given in the figures. Scale bar given in panel (i) applies to panels A–I & a–i, scale bar given in panel (p) applies to panels K–P & k–p, they represent approximately 100 μm.